2010

"A Pilot Study to Determine Shear-Wave Velocities for Earthquake Site Response at Cal Poly Pomona Campus using Refraction Micro-Tremor"

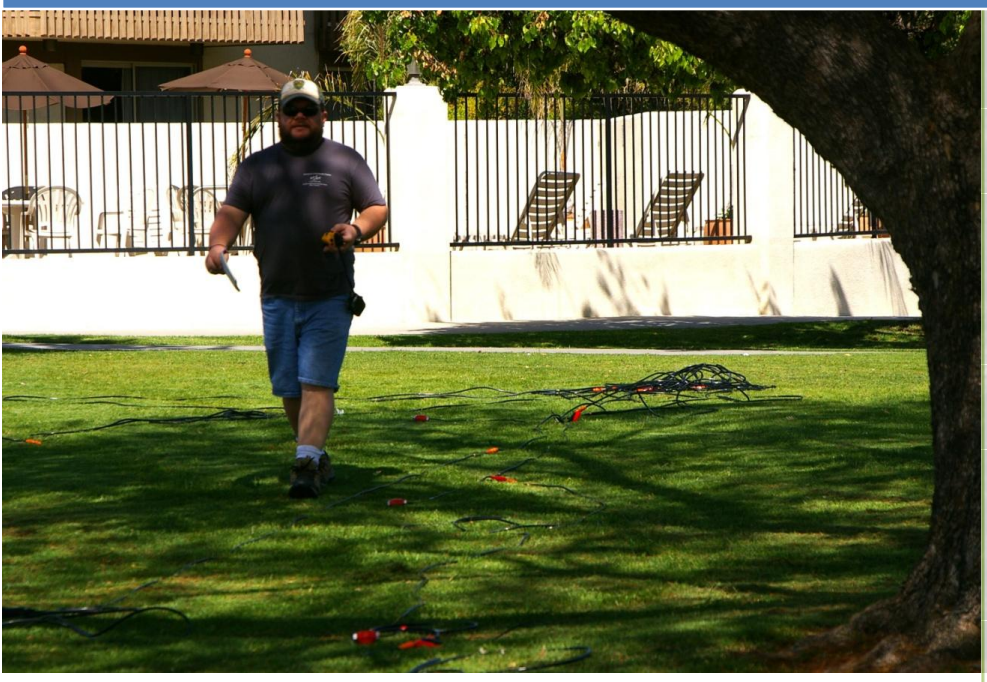

Brian Oliver

Cal Poly Pomona

5/4/2010

“A Pilot Study to Determine Shear-Wave Velocities for Earthquake Site Response at Cal Poly Pomona Campus using Refraction Micro-Tremor (ReMi)”

By
Brian Oliver
Geological Sciences Department
California State Polytechnic University
Pomona, Ca

2010 Senior Thesis
Submitted in Partial Fulfillment
of Requirements for a
B. S. Degree in Geology
Advisor
Dr. Jascha Polet

Table of Contents

Abstract **4**

Motivation **5**

ReMi **5**

Method **6**

Rayleigh Waves and Dispersion **6**

Equipment **7**

Data **7**

Site Location **7**

Data Gathering **8**

Data Processing **8**

Results and Interpretation **10**

Final Vs30 Models **10**

2003 Study **11**

Conclusion **12**

Appendix A **13**

Appendix B **14**

Appendix C **15**

Appendix D **17**

Works Cited **27**

Abstract

The need for a simple effective method for determining on-site analysis of shallow subsurface shear wave velocity structure has become more important as our understanding of earthquakes increases. The problem with determining these shallow shear wave velocity structures is that many of the areas we need to examine have structures already in place and are in areas which are polluted with ambient seismic noise. Previous methods for determining the shallow shear wave velocity structure of a given subsurface has either required drilling or "seismically quiet" time periods in which to perform the analysis. This becomes increasingly difficult in populated areas. To overcome this problem, a method has been developed to use the "seismic noise" or micro-tremors to map the shallow shear wave velocity structure. This is known as the ReMi (Refraction Micro-tremor) method.

The intent of this paper is to conduct a pilot study of the ReMi method on the campus of Cal Poly Pomona. The campus is home to thousands of students and faculty. This fact increases the importance of increasing our knowledge of the seismic hazard on campus. The knowledge can be used to identify areas of increased hazard and to minimize the potential damage and loss of life on campus by identifying the International Building Code (IBC) site class for two separate locations on the campus. Due to the location on campus, a non-invasive method of determining the shallow shear wave velocity structure was chosen. Since the campus is located near the interchange of two major freeways and is inhabited by students, it limited our choices for performing the analysis. The use of explosives was determined to be both dangerous and disruptive to the community, drilling was cost prohibitive, and due to the seismic pollution presented from the freeways all other methods became unsuitable for this task. The answer to the problem became apparent when the ReMi method was discovered. The micro-tremors produced from normal activities about the campus and freeways could be used to map the shallow shear wave velocity structure about the campus. The results of the pilot study demonstrated that the ReMi method can effectively be used to provide accurate shallow shear wave velocities, which can be used to determine the IBC site classification.

Motivation

Purpose and Objective: The purpose of this paper is to conduct a pilot study to determine the shear-wave velocities for earthquake site response on the campus of Cal Poly Pomona using the refraction micro-tremor method (ReMi). This shear-wave velocity (Vs30) for the upper 30 meters of the sub-surface is important for geotechnical assessments of earthquake site response. The shear-wave velocity is used to determine the International Building Code (IBC) site classification (Figure 1).

IBC 2006 Table 1613.5.2
SITE CLASS DEFINITIONS

SITE CLASS	SOIL PROFILE NAME	AVERAGE PROPERTIES IN TOP 100 FEET, SEE SECTION 1613.5.5		
		Soil shear wave velocity, v_s, (ft/s)	Standard penetration resistance, N	Soil undrained shear strength, s_u, (psf)
A	Hard Rock	$v_s > 5{,}000$	N/A	N/A
B	Rock	$2{,}500 < v_s \leq 5{,}000$	N/A	N/A
C	Very dense soil and soft rock	$1{,}200 < v_s \leq 2{,}500$	$N > 50$	$s_u \geq 2{,}000$
D	Stiff soil profile	$600 \leq v_s \leq 1{,}200$	$15 \leq N \leq 50$	$1{,}000 \leq s_u \leq 2{,}000$
E	Soft soil profile	$v_s < 600$	$N < 15$	$s_u < 1{,}000$
E	--	Any profile with more than 10 feet of soil having the following characteristics: 1. Plasticity index PI > 20, 2. Moisture content w ≥ 40%, and 3. Undrained shear strength s_u < 500 psf		
F	--	Any profile containing soils having one or more of the following characteristics: 1. Soils vulnerable to potential failure or collapse under seismic loading such as liquefiable soils, quick and highly sensitive clays, collapsible weakly cemented soils. 2. Peats and/or highly sensitive clays (H > 10 feet of peat and/or highly organic clay where H = thickness of soil) 3. Very high plasticity clays (H > 25 feet with plasticity index PI > 75) 4. Very thick soft/medium stiff clays (H > 120 feet)		

For SI: 1 foot = 304.8 mm, 1 square foot = 0.0929 m^2, 1 pound per square foot = 0.0479 kPa. N/A = Not applicable

Figure 1. International Building Code Site Classification Definitions.

The classification system is based on Vs30 measurements. These measurements are an average of the individual velocity layers within the top 30 meters of the subsurface, which helps engineers using the classification system to define the seismic hazard. This classification then contributes to the reduction of earthquake losses like those of the 1989 Loma Prieta earthquake, which encountered serious ground motion amplification (Figure 2).

The importance of an accurate subsurface model for earthquake response can help engineers design and retrofit structures that can withstand ground motions that may be amplified by near-surface shear-wave velocities. It is also of importance for emergency planners. It allows emergency response agencies and city planners, whether they are Federal, State, County, or City, design response plans according to the amount and location of expected damage due to high amounts of ground motion shaking.

Figure 2. Courtesy of **C.E. Meyer, , U.S. Geological Survey. Picture Take 10/19/1989. Ground view of collapsed building and burned area, Beach and Divisadero Streets, Marina District, San Francisco, CA, USA**

Site Class and Amplification: It has been shown through earlier studies that a correlation exists between site classification and amplification of ground motion (Stewart, et al. 2001). The correlation shows that high Vs30 measurements correlate with lower amplifications, while low Vs30 measurements correlate with high amplification. The correlation is shown as in Figure 3 (Stewart, et al. 2001). It is the averaged spectral amplification vs. *Vs-30,* taken from data collected from 37 sites in the San Francisco Bay region that recorded the 1989 Loma Prieta earthquake.

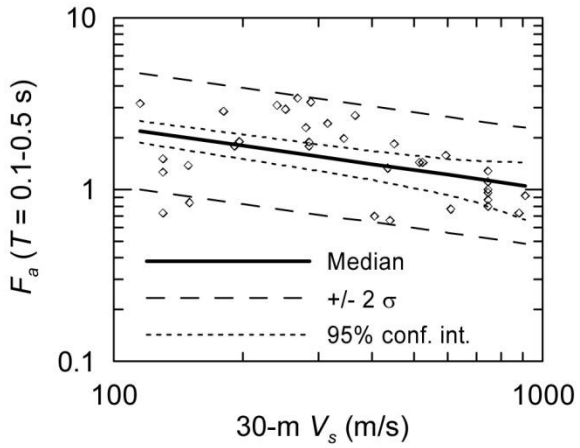

Figure 3 Averaged spectral amplification vs. Vs 30 for 37 sites in the San Francisco Bay region that recorded the 1989 Loma Prieta earthquake. (Stewart, et al. 2001)

ReMi: The ReMi method involves the use of standard P-wave refraction equipment to measure

the average shear wave velocity, anywhere from 40 meters down to a depth of 100 meters (Rucker 2007). This new method is performed at the surface in a non-invasive manner using ambient seismic "noise" of microtremors. The ambient seismic noise is generated from both cultural and natural sources. The surface wave dispersion is measured at the surface and inverted to create an average shear wave velocity model (Kaiser and G. 2005).

Advantages of ReMi: The ReMi method is not the only available method to measure Vs30 values. Other methods such as the Borehole Method, Spectral Analysis of Surface Waves (SASW), and Multichannel Analysis of Surface Waves (MASW) also exist, but the ReMi method demonstrates clear advantages over the other methods. The ReMi method is more efficient, less expensive, requires less permitting (if any at all), and uses ambient seismic noise.

Since the ReMi method uses standard P-wave refraction equipment deployed in a simple linear array, it saves time and money. It saves time over the borehole method, the SASW (Songyu, Lei and Xiaojun 2006), and the MASW (Park, Miller and Xia 1997). These methods require either time consuming drilling or consistently changing seismic arrays. The simplicity of the deployment means that the experiment can be done in a minimum amount of time. From deployment to result can be done within a 3 hour time frame.

The simple seismic array and equipment deployment also minimize site restrictions. The ReMi method only requires a linear distance of about 100 meters to deploy the seismic array, which is easier that using the more complicated SASW and MASW, or drilling equipment. This opens up many sites previously not considered. In fact, the equipment is minimal and can even be backpacked into remote sites. Another common site restriction is due to ambient seismic noise at the site. The noise interferes with other two surface wave measurement techniques. This isn't the case for ReMi, because it uses the ambient seismic noise as its source. This again opens up sites or saves money, by not requiring a site be shut down during the experiment. An example would be an active construction site or an airport in use.

Method

Rayleigh Waves and Dispersion: Up to this point, we have discussed the fact that ReMi uses standard P-wave refraction equipment and relies on ambient noise to measure surface wave, but what type of surface waves does the technique detect and how do these surface waves interact with the subsurface? The answer is Rayleigh waves which are dispersive waves.

Rayleigh waves are surface waves commonly known as "ground roll." The waves consist of both P-wave and S-wave components (Figure 4). The motions of particles near the surface of these waves undergo retrograde elliptical motion, which changes to prograde motion at depth (Shearer 1999). In addition to the different particle motion with depth, the wave also undergoes dispersion.

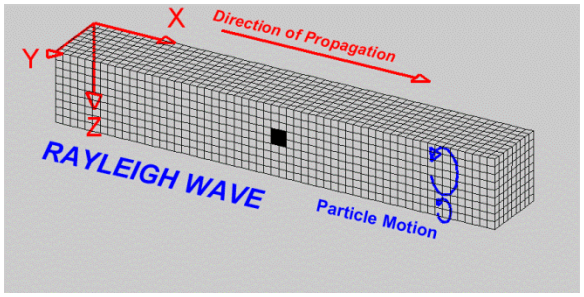

Figure 4. Diagram demonstrating the motion of Rayleigh Waves.

Dispersion in Rayleigh waves means that velocity is not constant and varies with wavelength (Burger, Sheehan and Jones 2006). In other words, different frequency components of a wave travel at different speeds. This is important because these different period (inverse of frequency) waves are sensitive to different depths. Longer periods are more sensitive to deeper structure, so we measure velocity as a function of period and invert for velocity structure.

Equipment: The equipment used in this pilot study was a simple P-wave refraction set. It consisted of:

1. 12 Geophones (4.5Hz)
2. 2 Geophone Cables
3. Data Logger
4. Battery Pack
5. Laptop

The equipment was deployed in a linear array with the data logger and battery in between the two geophone cables. On either side of the data logger 6 geophones were attached to the geophone cable and coupled securely with the ground. The data logger consists of two seismographs with each seismograph able to recognize 6 geophones, hence the design of our experiment. Attached to one end of a geophone cable, the laptop or recording device was attached. The software used was SeisOpt ReMi (Louie 2003).

Figure 5. Standard P-wave Equipment including Laptop, Data Logger, Battery, Geophone Cable, and Geophone.

Data

Site Location: Two sites on the campus of Cal Poly Pomona were chosen for contrast. The first site was on the east end of the campus and the second on the west end. The following picture identifies each site (Figure 6).

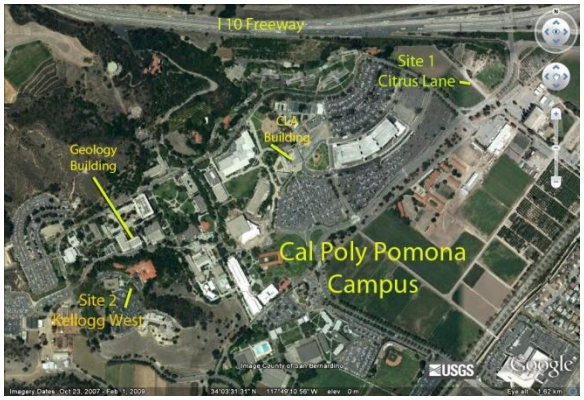

Figure 6. Google Earth Image showing location of experiments on the Cal Poly Pomona campus.

Site one was located along an access road, which accessed horse meadows. According to the California State Geological Map, the meadows are located upon alluvial fill, which is unconsolidated to semi-consolidated, and are situated south of the I 10 freeway and west of the 57 freeway. The red line represents the geophone array deployed at this site (Figure 7).

Figure 7. Google Earth Image of site one showing location of seismic array deployment.

Site two was located on a hill which consisted of moderately to well consolidated marine sediments. The seismic array was deployed on a grass lawn next to a parking lot and hotel (Figure 8). Here the red line represents the seismic array deployment.

Figure 8. Google Earth image of site two showing location of seismic array deployment.

Data Gathering: The experiments conducted at each site were implemented using different seismic sources. This was done to investigate whether or not different seismic sources had any impact on the results.

The first site (Figure 9) was deployed along the road between the meadows. The length of the seismic array was 120 meters, with 12 geophones spaced 10 meters apart. This arrangement was then used to record a total of 12 experiments with trace lengths of 32 seconds. The first five experiments were recorded using the ambient seismic noise, a truck, and one blow from a sledgehammer upon a metal plate. The truck was a Nissan Frontier, which was driven along the seismic array while recording. Next, we conducted five more experiments without the sledgehammer, but still drove the truck along the array. Finally, two more experiments were done using only the ambient seismic noise.

Figure 9. Image of site one with seismic array deployed along the road.

The second site (Figure 10) was similarly deployed with modification. The site length was half of site one and required us to deploy the seismic array differently. The total length available was just over 60 meters. This means that we were forced to shorten our deployed array to 60 meters and modify the geophone spacing to 5 meters. This way we were able to deploy all 12 geophones. The trace length was still 32 seconds, but a total of 14 experiments were conducted here. Again we varied the seismic sources to test if the source would affect the result. The first experiment recorded at site two was done with only ambient seismic noise. The second two experiments were done with the ambient seismic noise and me walking along the deployed array. Finally, for the next eleven experiments, we recorded ambient seismic noise and used my truck again to drive along the array within the parking lot.

Figure 10. Image of site two with seismic array deployed on the grassy lawn.

Data Processing: Once the data was collected, it was processed using the SeisOpt ReMi software. This software converted the data into "planes" or p-f images. Each individual experiment was transformed into a plane. The plane is a plot showing the arrival time of seismic energy as a function of slowness and frequency (Figure 11). The color differences represent different energy levels or amplitudes. The red colors represent higher amplitudes and the blue colors lower amplitude.

Recalling that we are measuring the arrival times of Rayleigh waves of different periods, which are sensitive to different depths, we can use these measurements of Rayleigh wave dispersion to invert

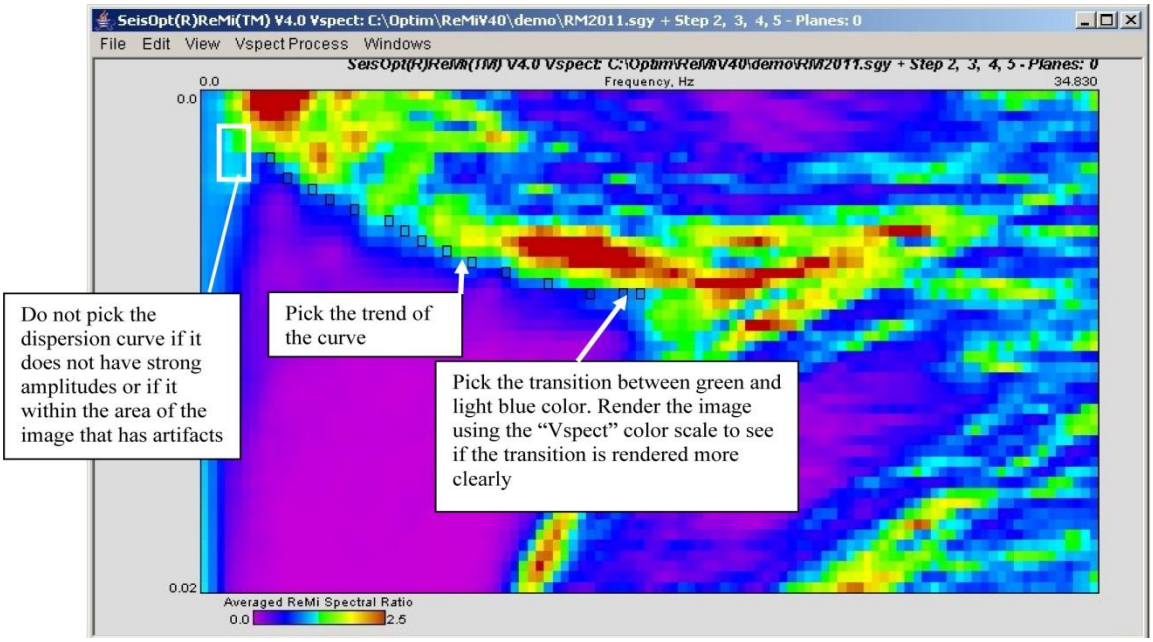

Figure 11. Courtesy of Optim Software and Data Solutions SeisOpt ReMi software Manual. The figure demonstrates how the dispersion curve is picked. The "picks" are black boxes along the dispersion curve boundary.

for a model of velocity with depth. Of course we first need to stack the various planes to improve the signal to noise ratio. For the various planes see Appendix A.

After the various planes were created, the planes were stacked in various combinations. At site one, the first five planes were stacked as a stacked plane. This means that only the first five planes at site one, which shared common seismic sources, were stacked. This was also done for the second five planes, the last two, and finally all planes from the site were stacked. This again was done to test the idea that seismic source may have an effect on the results. Planes were also stacked according to seismic source at site two, as well. For the various stacked planes see Appendix B.

Once the stacked planes were created, the planes were manually "picked". The stacked planes were picked along the lowest energy bound of the high amplitude trend. Meaning that at the color boundary, light blue and green, a "pick" was chosen to represent the actual velocity or slowness at that frequency (Figure 12). The lower energy bound was chosen to avoid the apparent velocity in the high amplitude trend. The high amplitude trend is always the trend sloping downward from the left.

Once the picked planes were created, the picked plane was inverted to create velocity models, using the software. Each picked plane resulted in a model with an associated dispersion curve (Figure 13).

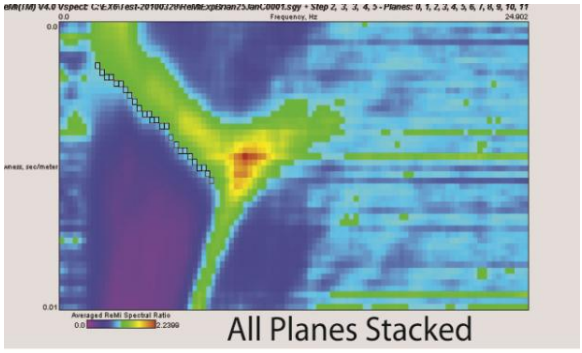

Figure 12. The "Picks" for site one.

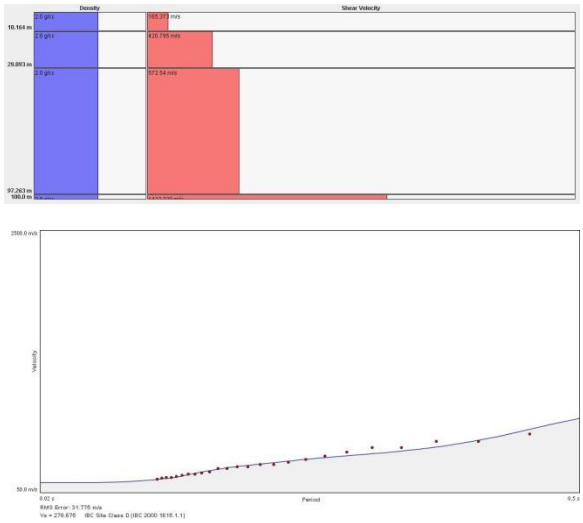

Figure 13. Site One 4 Layer Dispersion Curve and Model.

At this point, velocity models were created and inversions were carried out for models with different numbers of layers to see if the choice of number of layers had an effect had an effect on the Vs30 values determined. Each stacked and picked plane from site one was modeled using anything from 3 to 8 layers. At site two, the stacked and picked planes were modeled using 3 to 6 layers. The different layers were modeled and the resultant Vs30, site class and fit to the dispersion curve were tested. For all the various velocity models and their associated dispersion curve see Appendix C.

Results and Interpretation

Final Vs30 Models: The results from each velocity model indicated that the Vs30 and therefore the site classification were independent of the seismic source used or details of the chose input parameters for the velocity model inversion. The Vs30 and sit class remained consistent. Because of this, the stacked and picked planes used to determine the final Vs30 and site classification were the all planes stacked planes. This meant that for each site, all experiments were stacked and then picked (Figure 12 and 15). Ultimately, the velocity models inverted for were visually inspected and chosen by the following criteria. I decided that the simplest velocity model that fit the associated dispersion curve would be our model. I avoided velocity models with very thin layers and any multiple layers of similar velocity. The results were a 4 layer model (Figure 13) for site one and a 3 layer model (Figure 16) for site two. All other results from the various velocity models can be found in Appendix D.

Site 1 Horse Meadow			
Geophone Spacing			10 meters
Number of Geophones			12
Number of Experiments			12
All Planes Stacked			
Layers	Error (m/s)	Vs30 (m/s)	IBC Site Class
3	59.329	293.468	D
4	31.775	278.675	D
5	56.684	286.948	D
6	28.212	278.679	D
7	12.03	250.573	D
8	10.901	271.156	D

Figure 14. Table showing the Vs30 results for various layered models.

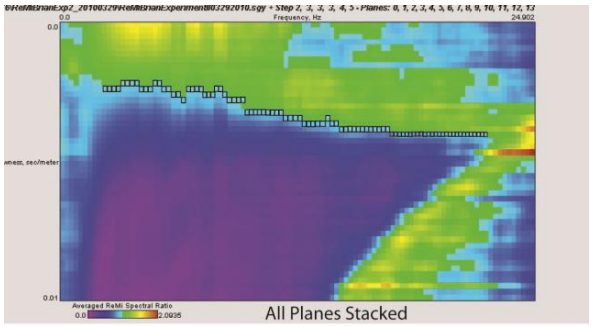

Figure 15. The "Picks" for Site Two.

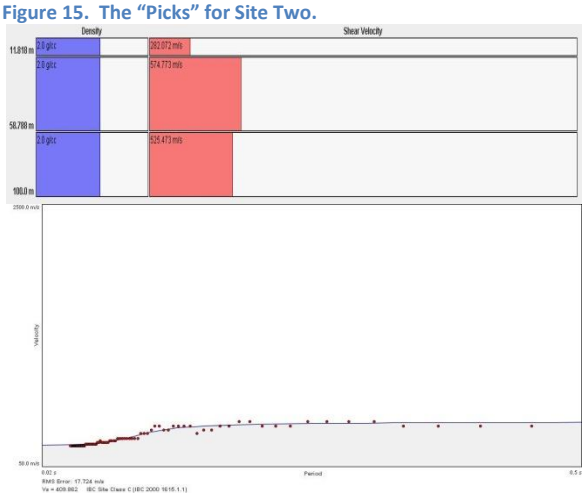

Figure 16. Site Two 3 Layer Dispersion Curve and Model.

For site one, the Vs30 values ranged from 251 m/s to 294 m/s (Figure 14). This range of Vs30 values are well within the limits of a site class of D. The number of layers did not have an effect on the Vs30 values and therefore the site classification. For site two, similar results were obtained. In this case, the Vs30 values were between 404 m/s and 410 m/s (Figure 17). The range of values here was even smaller, and remained within the range of Vs30 values consistent with a site classification of C. Again the details of the model were irrelevant but the difference in site classes between sites supported the idea that differing geologies affect the amplification of shaking. Surfaces of the Earth where more consolidated rock, like that found at site two, should have less ground shaking than that of more like unconsolidated layers those of the alluvial fill at site one.

Site 2 Kellogg West			
Geophone Spacing			5 meters
Number of Geophones			12
Number of Experiments			14
All Planes Stacked			
Layers	Error (m/s)	Vs30 (m/s)	IBC Site Class
3	17.724	409.862	C
4	17.057	404.572	C
5	16.722	407.891	C
6	17.247	404.12	C

Figure 17. Table showing the Vs30 results for various layered models.

2003 Study : Finally, in 2003, the University of Reno's Seismological Laboratory was contracted to conduct a large scale study of site classifications around Southern California. One of the constraints they used to determine their experiment sites was that the experiment site must be within 200 meters of a ground motion recording site. One of these sites CPP was on the campus of Cal Poly Pomona (Figure 18) . The ground motion recording site was only 400 meters away from site one (Louie 2003). The sites shared a similar geology, where both sites were on top of alluvial basin fill. The results from the Reno study were a match for the results at site one (Figure 19). The two independent experiments confirm the determined Vs30 values and site classification.

Figure 18. Google Earth image of Cal Poly Pomona campus showing location of University of Renos experiment site.

Table 1 summarizes measurement array center locations, distance from the CISN station assessed, and our resulting average velocities to 30-, 50-, and 100-meter depths, denoted Vs30, Vs50, and Vs100, respectively.

Sta	Meas. Lat	Meas. Lon	Dist to Sta, m	Vs30, m/s	Vs50, m/s	Vs100, m/s
AGO	34.146430	-118.766275	82	410	474	545
CHN	33.999025	-117.679810	18	315	381	474
CLT	34.093060	-117.316360	53	306	377	509
CPP	34.059520	-117.808700	60	279	332	399
CRN	33.876030	-117.560305	64	340	382	421
DEC	34.253410	-118.332795	129	452	548	734
DJJ	34.103990	-118.454270	225	337	380	428
FMP	33.712115	-118.292425	176	351	411	492
GR2	34.123490	-118.296260	660	417	538	715
GSA	34.136590	-118.127810	49	338	386	499
HLL	34.174290	-118.359570	238	304	347	404
LAF	33.869959	-118.333781	247	281	311	339
LBW2	33.798396	-118.088072	52	279	311	368

Figure 19. Table summarizing the University of Reno's experimental results and their distances from the CISN stations. (Louie 2003) See CPP for results at Cal Poly Pomona with a Vs30 of 279.

Conclusion

The results of the experiment from both site one and site two demonstrate that the Vs30 and site classification obtain through the ReMi technique appear to be in dependant of different seismic sources and model details. It didn't matter whether we used an artificially generated seismic source or the ambient seismic noise and it also didn't matter how many layers we used to fit the dispersion curve. Since all results for Vs30 remained consistent in all experiments, the site classification for each site was also constant. For site one, it was a site class of D and for site two it was a C. The results also were consistent with what I expected from the differing sites. Site was expected to have a better site classification than site one, because of the geology of that site. I expected that the more consolidated materials at site one should produce a superior site classification. The matching of the 2003 study results with those from site one were a nice check for validity and reliability. Both sites were located on similar geology and within 400 meters of each other. The very clear match between the two Vs30 results demonstrated that the ReMi technique provides reliable results.

Due to the fact that the experiment was completed with standard P-wave equipment, which most universities and geotechnical companies have, and it was done in a time efficient manner, with consistent results, the pilot study should be considered a success. The results in this pilot study support the idea that the ReMi method is a reliable technique to determine Vs30 values and site classification on campus in both an economical and time efficient manner.

Appendix A

"Planes"

Site One: Appendix A includes all planes from site one and site two. The planes directly to the right are all twelve experiments conducted at site one. The first column of planes includes the first five experiments, which were done with a sledge hammer, truck, and ambient seismic noise. The second column represents the second five experiments that represent the experiments conducted using only the truck driven along the array and the ambient seismic noise in the background. Finally, the last two planes in the far right column are experiments done with only ambient seismic noise.

Site Two: The experiments from site two are directly to the right. This is a total of fourteen experiments conducted with various seismic sources. The first plane, labeled plane one, was conducted with only ambient seismic noise. The next two planes were recorded using ambient seismic noise and me walking along the seismic array. Finally, the next eleven experiments were recorded using ambient seismic noise and my truck driven along the seismic array.

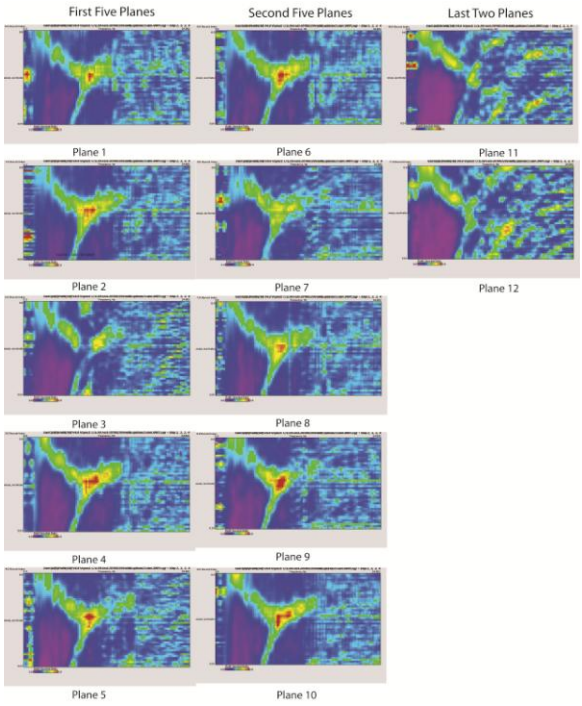

Figure A1. The Planes from Site One

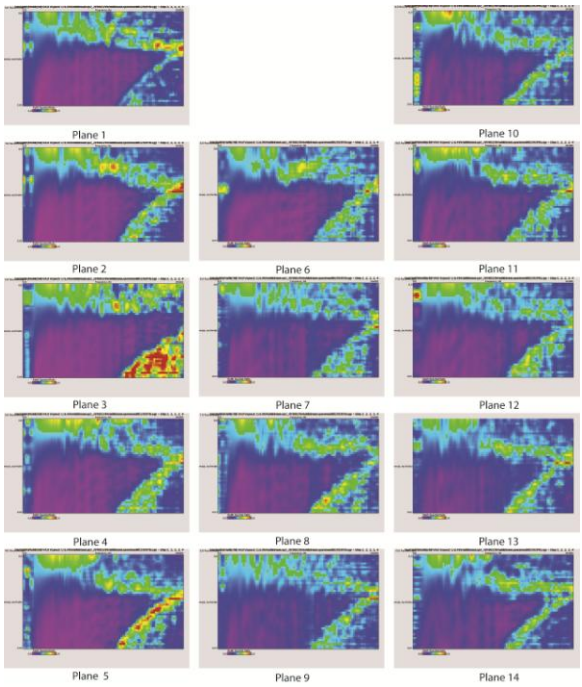

Figure A2 The Planes from Site Two.

Appendix B
"Stacked Planes"

Site One: The planes directly to the right are the various stacked planes. The planes were stacked according to their common seismic sources that were used to conduct the experiments. The top stacked plane is all twelve experiments conducted at site one. The next plane down is the first five experiments conducted and stacked. The third stacked plane is the second five experiments and finally the bottom stacked plane is the last two experiments conducted.

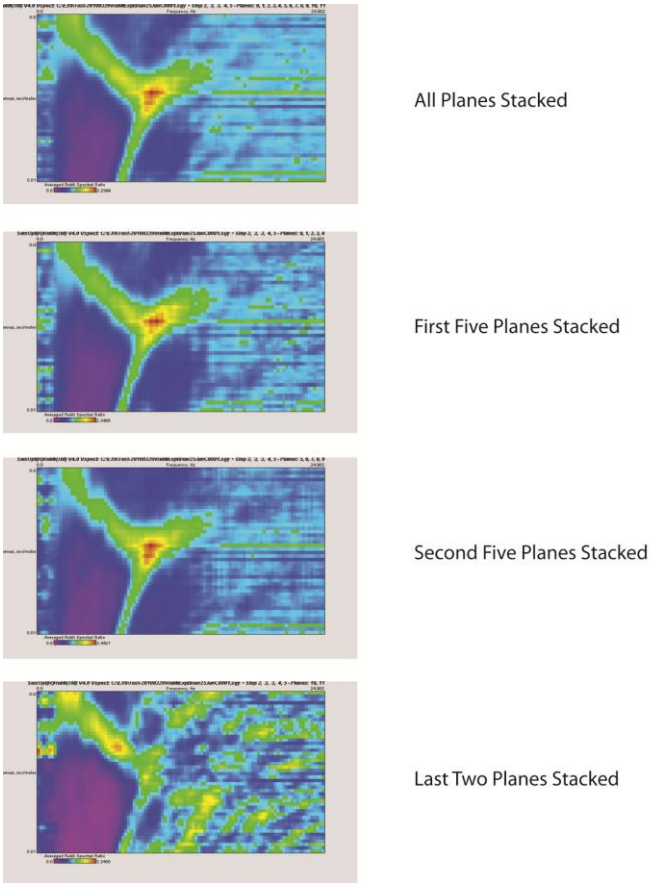

Figure B1. The Stacked Planes from different seismic sources.from Site One.

Site Two: The results from the first experiment demonstrated that the seismic source had no effect on the Vs30 and site class; therefore, we simply combined all fourteen experiments to determine the Vs30 and site classification.

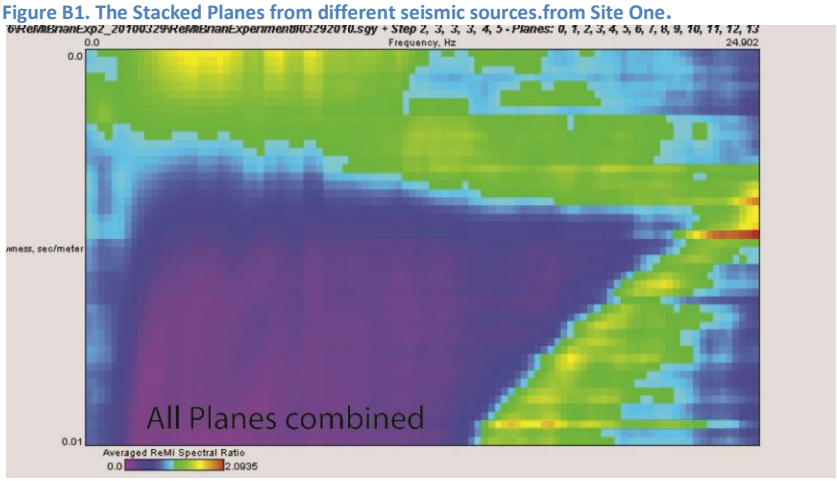

Figure B2. All planes were stack creating an all planes Stacked Plane.

Appendix C

"Picks"

Site One: The planes to the right are stacked planes showing the manually "picked" lowest energy bound of the high amplitude trend. The black squares are the manual picks.

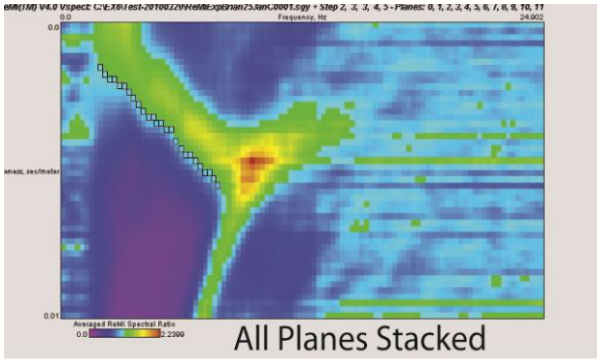

Figure C1. All Planes Stacked "Picks" Site One

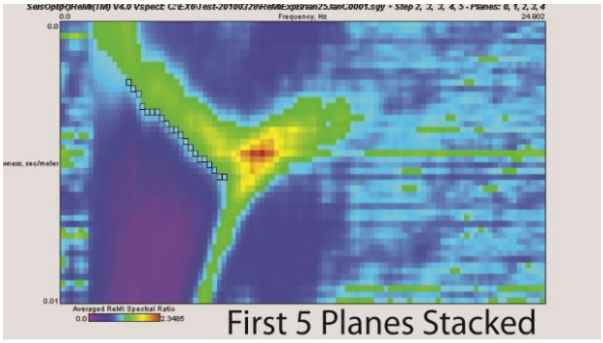

Figure C2. First Five Planes Stacked "Picks" Site One

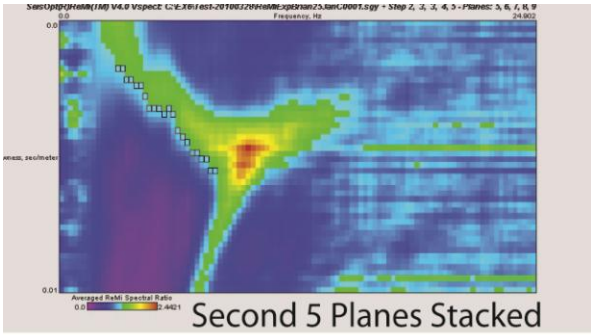

Figure C3. Second Five Planes Stacked "Picks" Site One

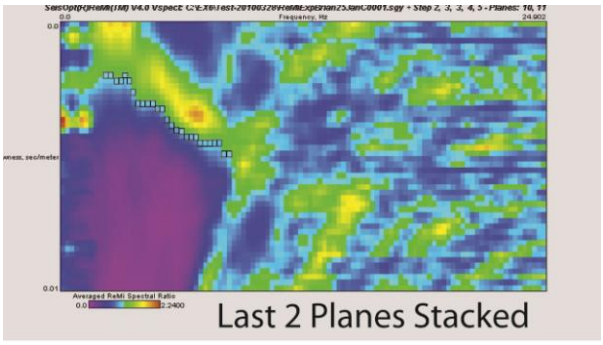

Figure C4. Last Two Planes Stacked "Picks" Site One

Site Two: The plane to the right shows the manual picks made to the high amplitude trend.

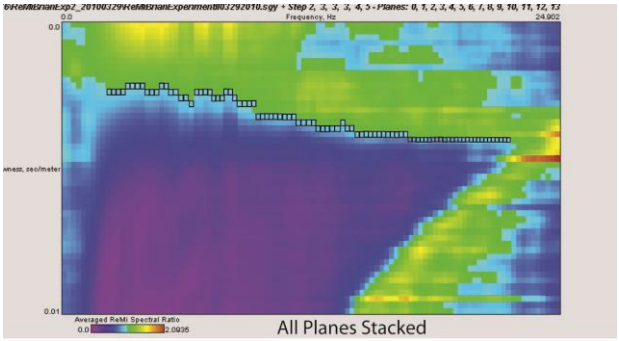

Figure C5. All Planes Stacked "Picks" Site Two.

Appendix D

"Models"

Site One: The following models are from site one. They show the various layered models with associated dispersion curve and results in table form.

First Five Planes Models

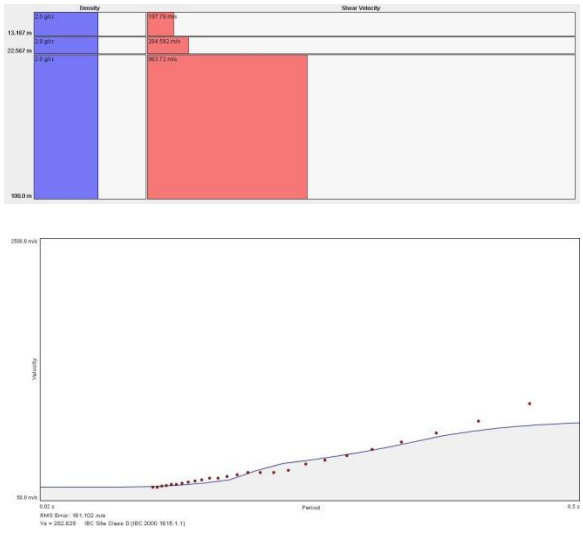

Figure D1. Three Layer Model for Site One

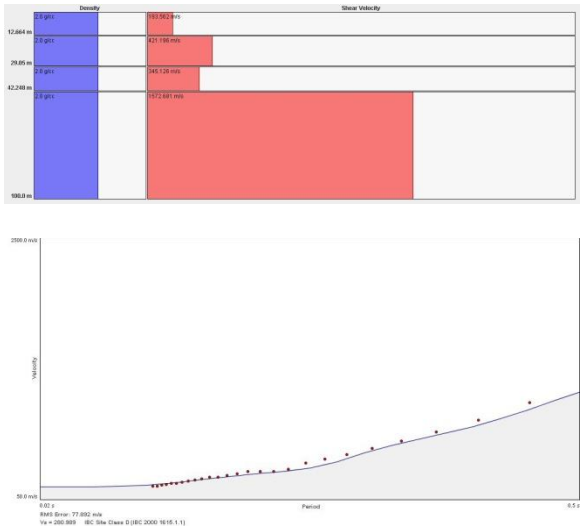

Figure D2. Four Layer Model for Site One

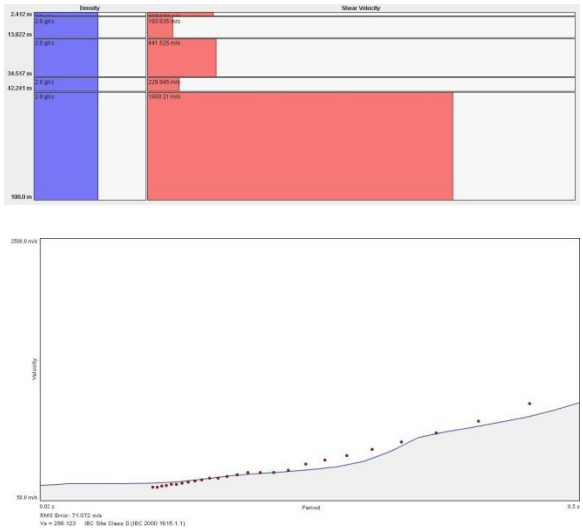

Figure D3. Five Layer Model for Site One

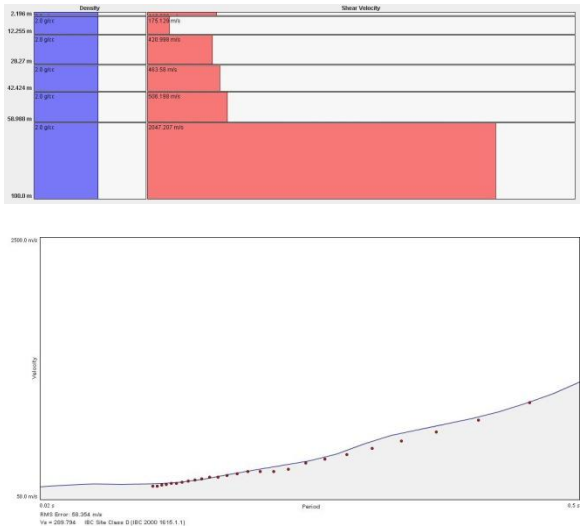

Figure D4. Six Layer Model for Site One

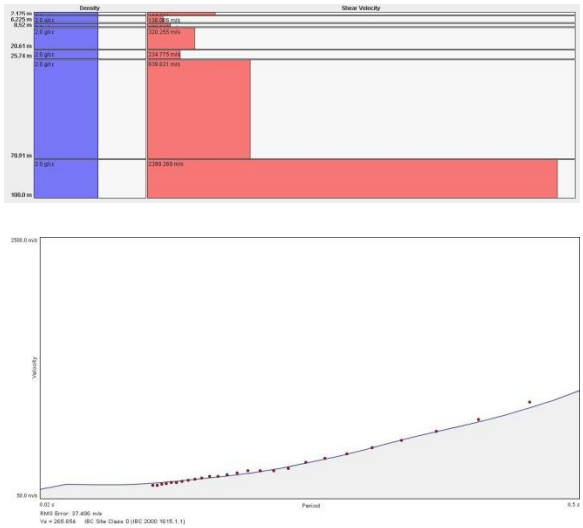

Figure D5. Seven Layer Model for Site One

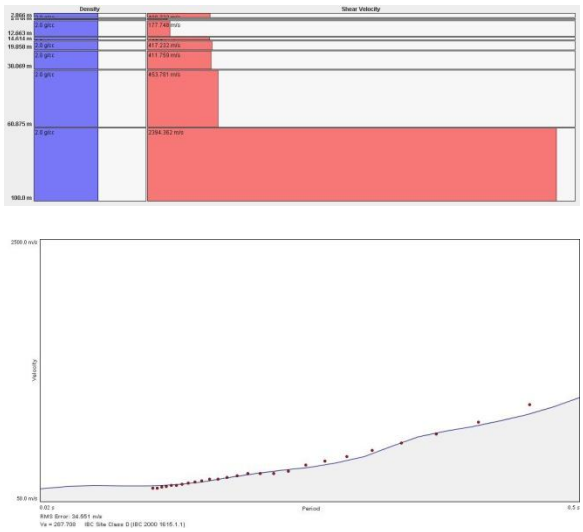

Figure D6. Eight Layer Model for Site One

Results for First Five Planes Models:

Site 1 Citrus Lane			
Geophone Spacing			10 meters
Number of Geophones			12
Number of Experiments			12
First Five Planes Stacked			
Layers	Error (m/s)	Vs30 (m/s)	IBC Site Class
3	161.102	252.629	D
4	77.892	280.989	D
5	71.072	298.123	D
6	58.354	289.794	D
7	37.486	265.654	D
8	34.551	287.708	D

Figure D7. Table to summarize the results from Site One Models of First Five Planes Stacked.

Second Five Planes Models

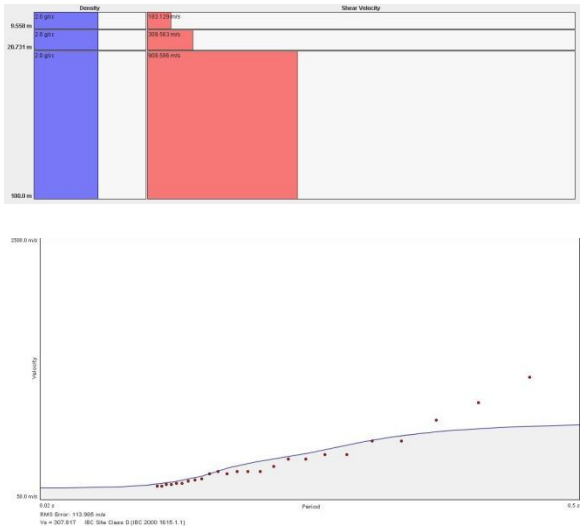

Figure D8. Three Layer Model for Site One

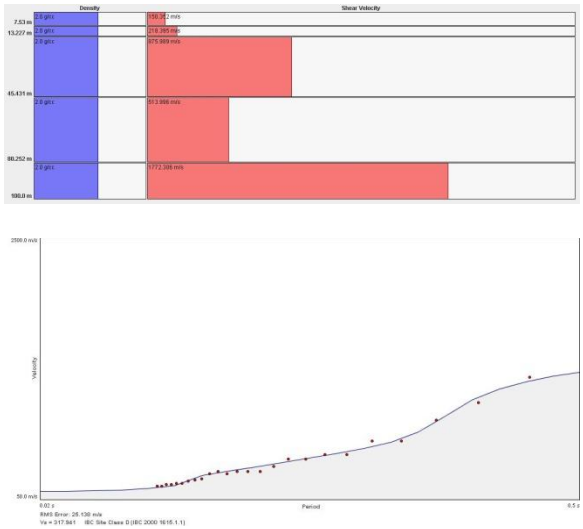

Figure D 10 Five Layer Model for Site One

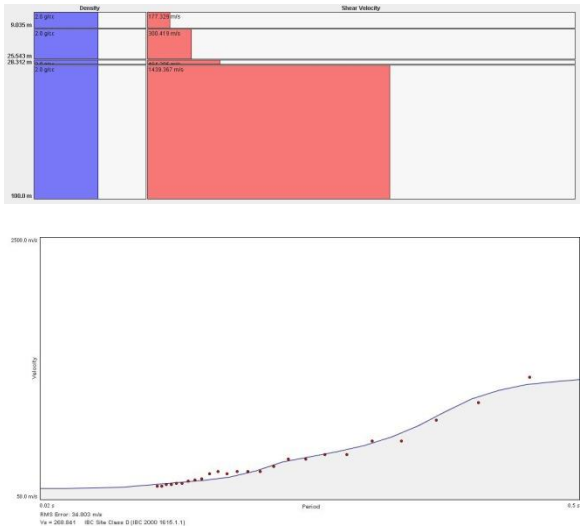

Figure D9. Four Layer Model for Site One

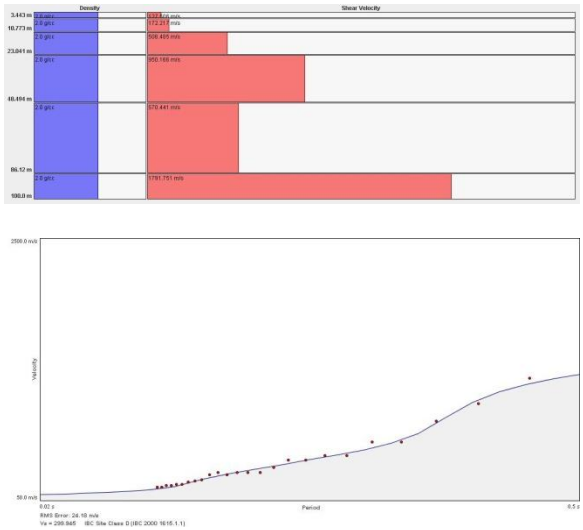

Figure D11. Six Layer Model for Site One

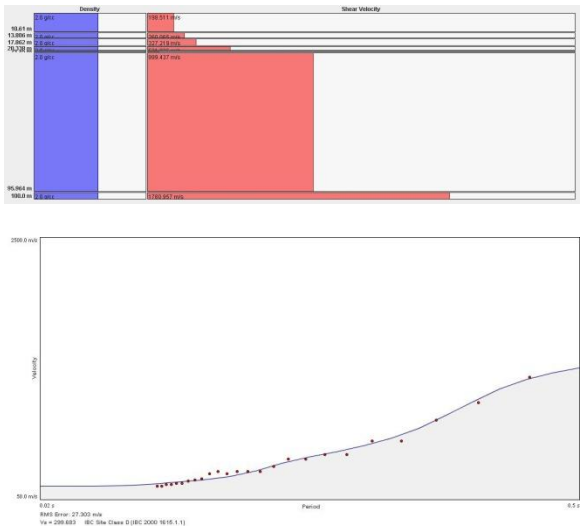

Figure D12. Seven Layer Model for Site One

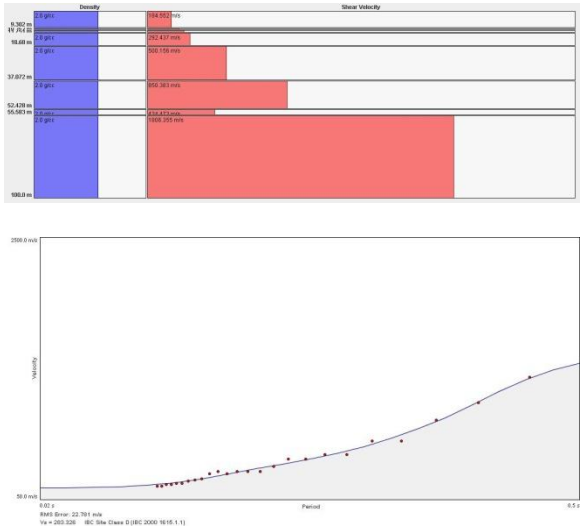

Figure D13. Eight Layer Model for Site One

Results for Second Five Planes Models:

Site 1 Citrus Lane			
Geophone Spacing			10 meters
Number of Geophones			12
Number of Experiments			12
Second Five Planes Stacked			
Layers	Error (m/s)	Vs30 (m/s)	IBC Site Class
3	113.985	307.817	D
4	34.803	268.841	D
5	25.138	317.941	D
6	24.18	299.945	D
7	27.303	299.683	D
8	22.781	283.326	D

Figure D14. Table to summarize the results from Site One Models of Second Five Planes Stacked

Last Two Planes Models

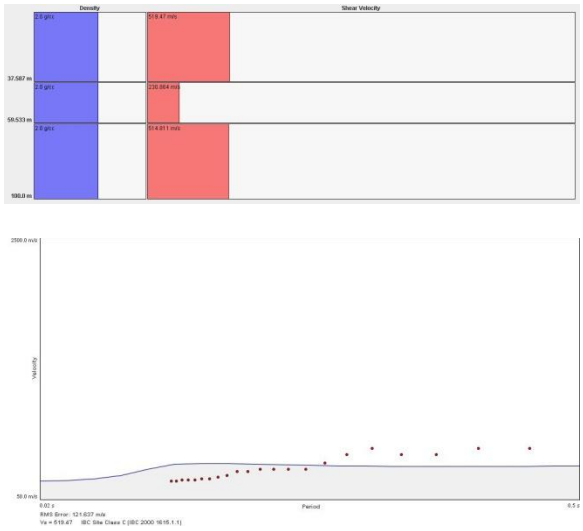

Figure D15. Three Layer Model for Site One

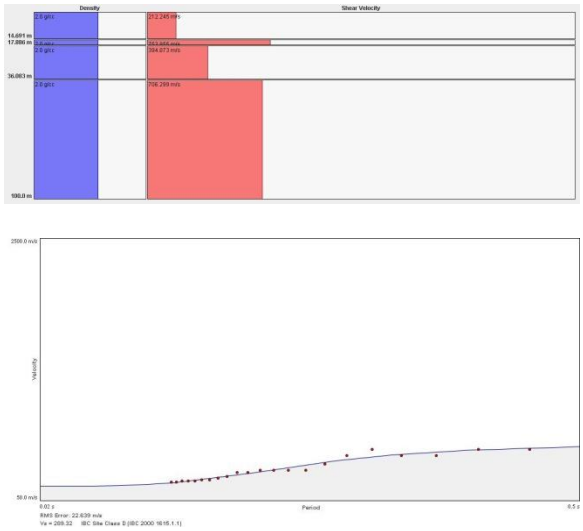

Figure D16. Four Layer Model for Site One

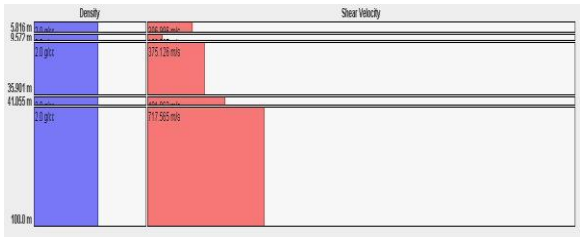

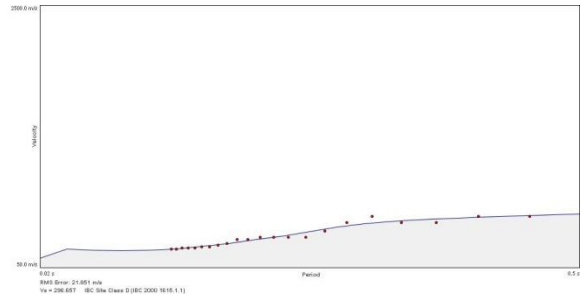

Figure D17. Five Layer Model for Site One

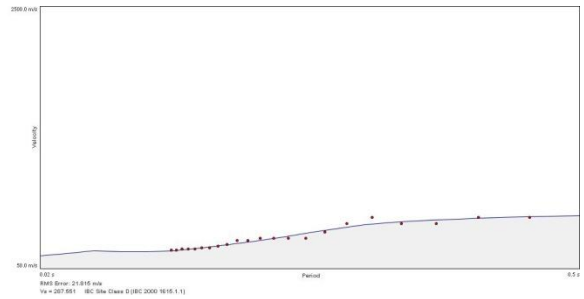

Figure D18. Six Layer Model for Site One

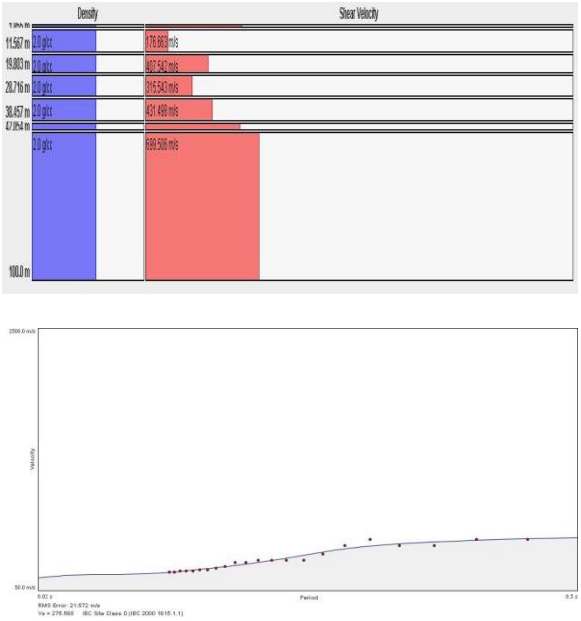

Figure D19. Seven Layer Model for Site One

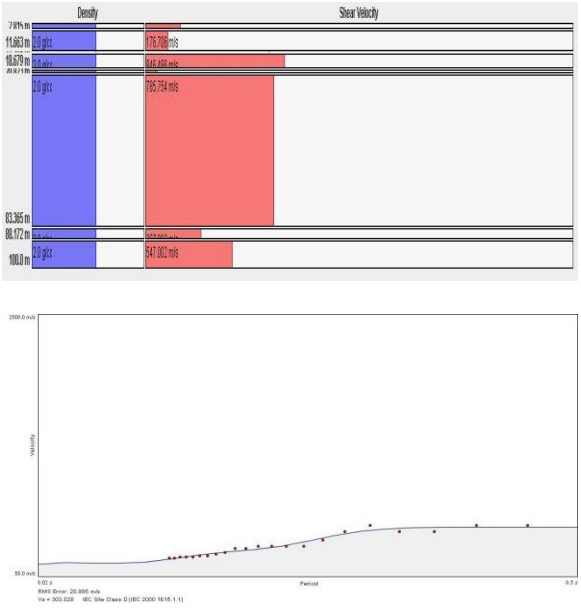

Figure D20. Eight Layer Model for Site One

Results for Last Two Planes Models:

Site 1 Citrus Lane			
Geophone Spacing			10 meters
Number of Geophones			12
Number of Experiments			12
Last Two Planes Stacked			
Layers	Error (m/s)	Vs30 (m/s)	IBC Site Class
3	121.637	519.47	D
4	22.639	289.32	D
5	21.851	296.657	D
6	21.815	287.551	D
7	21.572	275.568	D
8	20.885	303.028	D

Figure D21. Table to summarize the results from Site One Models of Last Two Planes Stacked

All Planes Models

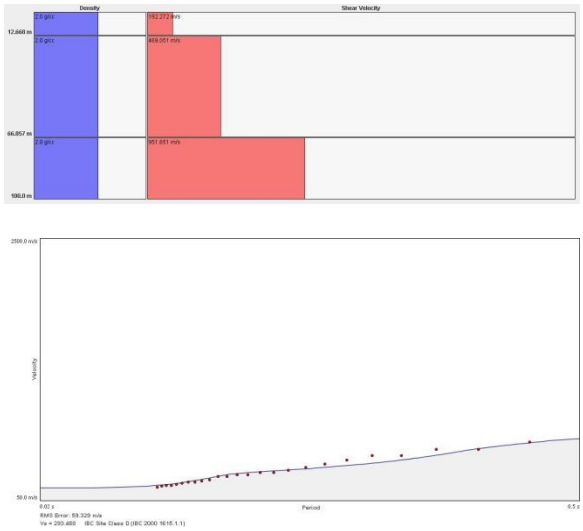

Figure D22. Three Layer Model for Site One

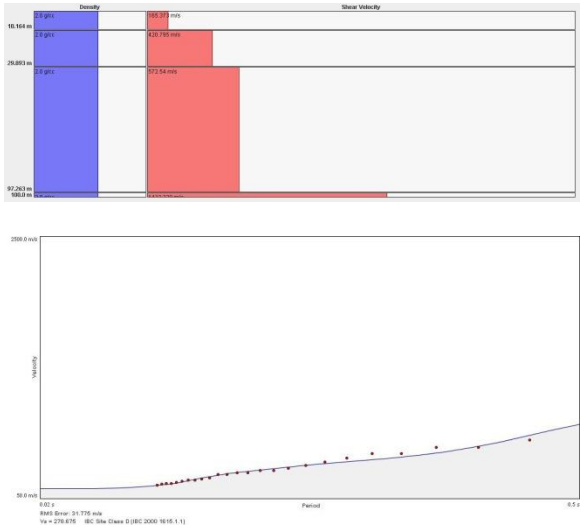

Figure D23. Four Layer Model for Site One

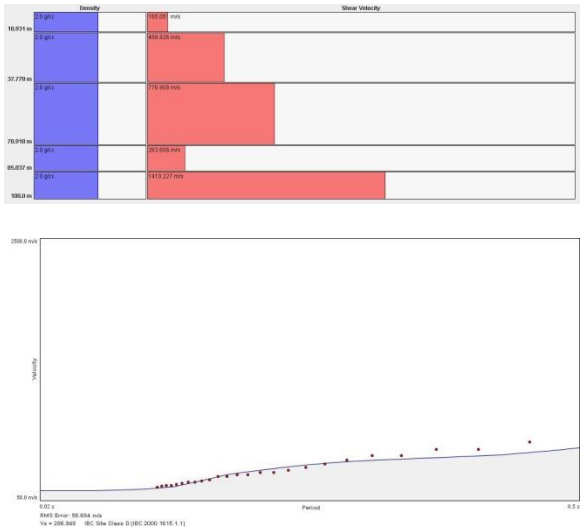

Figure D24. Five Layer Model for Site One

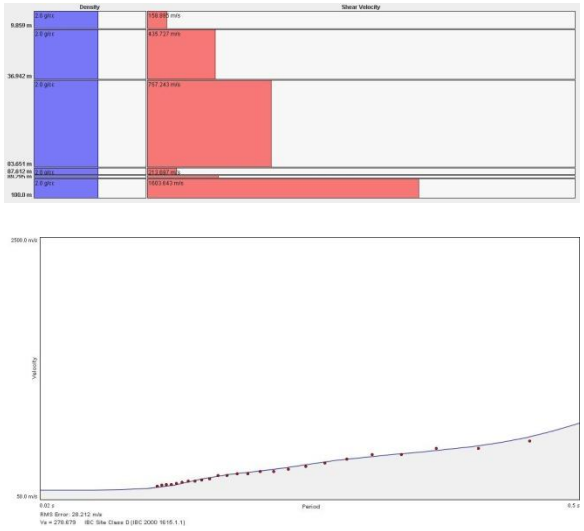

Figure D25. Six Layer Model for Site One

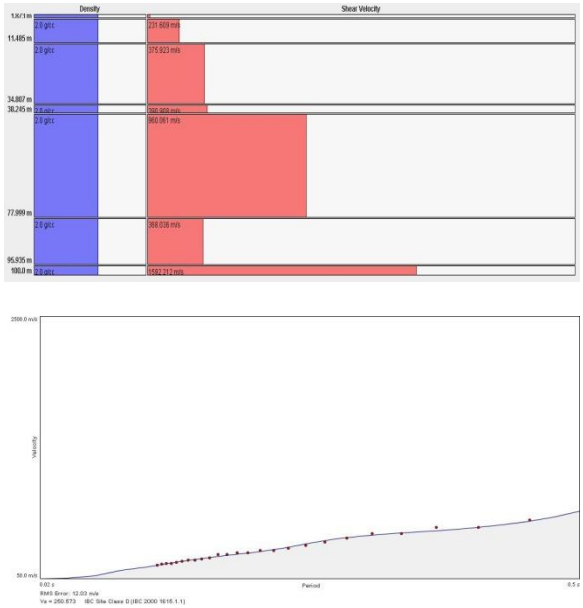

Figure D26. Seven Layer Model for Site One

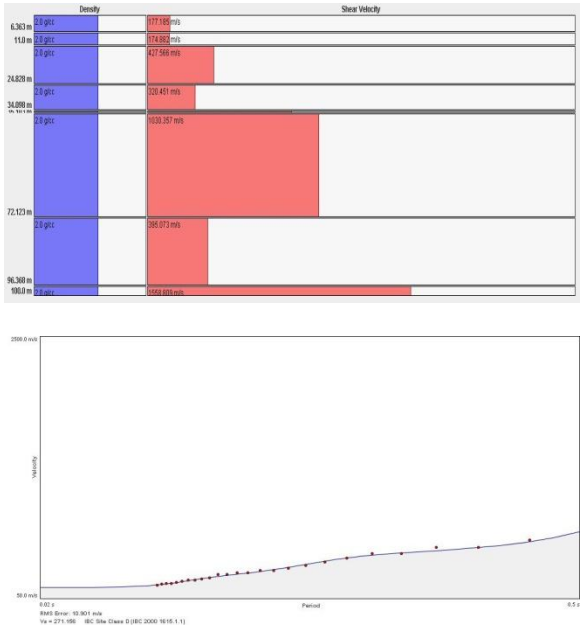

Figure D27. Eight Layer Model for Site One

Results for All Planes Models:

Site 1 Citrus Lane			
Geophone Spacing			10 meters
Number of Geophones			12
Number of Experiments			12
All Planes Stacked			
Layers	Error (m/s)	Vs30 (m/s)	IBC Site Class
3	59.329	293.468	D
4	31.775	278.675	D
5	56.684	286.948	D
6	28.212	278.679	D
7	12.03	250.573	D
8	10.901	271.156	D

Figure D28. Table to summarize the results from Site One Models of All Planes Stacked

Site Two: The following models are from site one. They show the various layered models with associated dispersion curve and results in table form.

All Planes Models

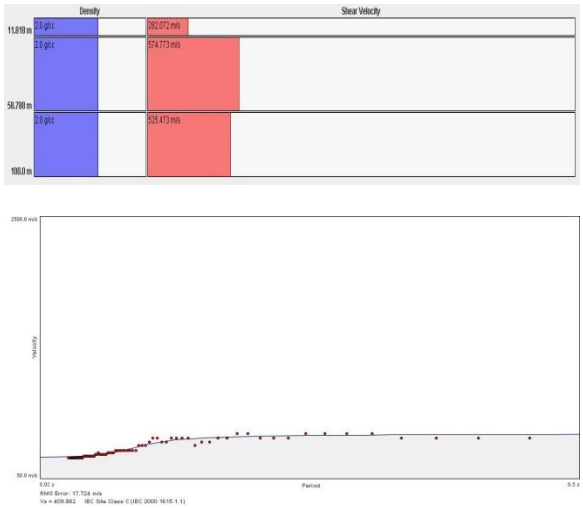

Figure D29. Three Layer Model for Site Two

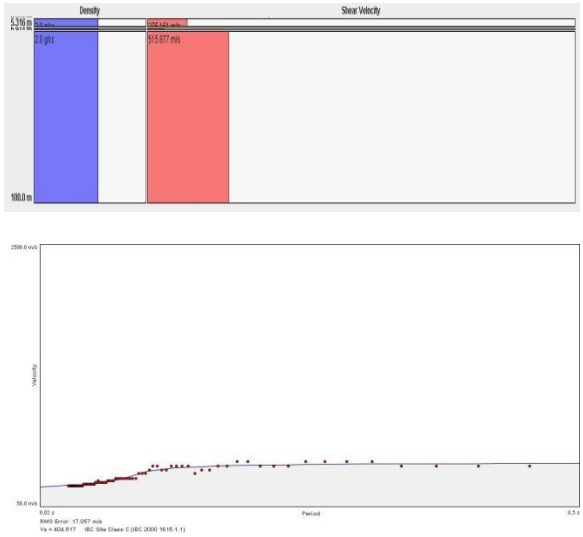

Figure D30. Four Layer Model for Site Two

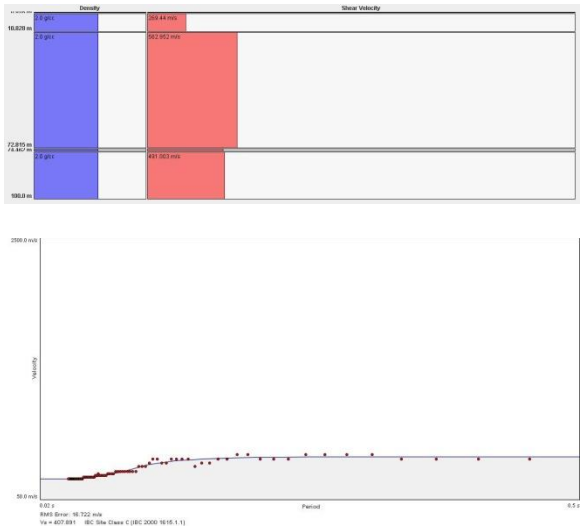

Figure D31. Five Layer Model for Site Two

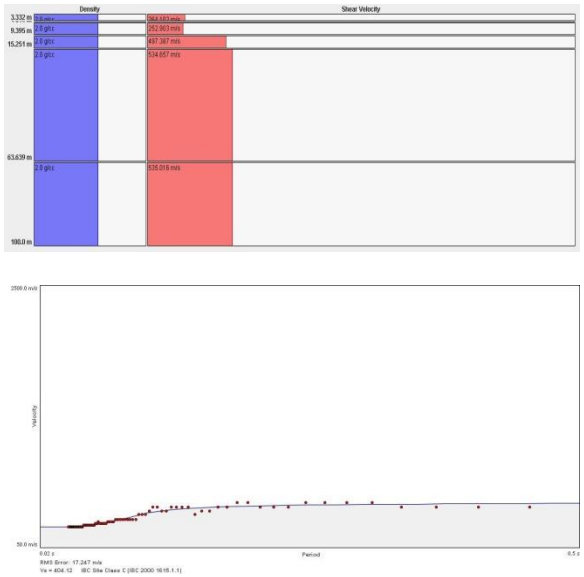

Figure D32. Six Layer Model for Site Two

Results for All Planes Models:

Site 2 Kellogg West			
Geophone Spacing			5 meters
Number of Geophones			12
Number of Experiments			14
All Planes Stacked			
3	17.724	409.862	C
4	17.057	404.572	C
5	16.722	407.891	C
6	17.247	404.12	C

Figure D33. Table to summarize the results from Site Two Models ofAll Planes Stacked

Works Cited

Burger, Robert H., Anne F. Sheehan, and Craig H. Jones. *Introduction to Applied Geophysics.* New York: W. W. Norton Company, 2006.

Kaiser, Anna E., and Smith Euan G. *Shallow Shear-Wave Velocity from ReMi Surface Wave Dispersion: Method and Case Study.* School of Earth Science,, Victoria University of Wellington, Wellington: , 2005.

Louie, John N. *Improving Next-Generation Attenuation Models with Shear-Velocity Measurements at All TriNet and Strong-Motion Stations in LA.* Technical, Reno: University of Nevada, 2003.

McPherson, A.A., and L.S. Hall. *Development of the Australian National Regolith Site Classification Map.* Record, Canberra: Australian Government, 2007.

Park, Choon, Richard Miller, and Jianghai Xia. *Multi-Channel Analysis of Surface Waves (MASW).* Summary report, Lawrence, Kansas: Kansas Geological Survey, 1997.

Rucker, Michael L. *Surface Geophysics as Tools for Characterizing Existing Bridge.* Tempe, Arizona: AMEC Earth & Environmental, Inc., 2007.

Shearer, Peter M. *Introduction to Seismology.* San Diego: Cambridge University Press, 1999.

Songyu, Liu, Fang Lei, and Yu Xiaojun. *Application of SASW in liquified Improvment.* Nanjing: Southeast University, China, 2006.

Stewart, Jonathan P., Andrew H. Liu, Choi YooJoong, and Baturay Mehmet. *Amplification Factors for Spectral Acceleration in Active Regions.* PEER Report 2001/10, Department of Civil and Environmental Engineering, University of California, Los Angeles, University of California, Berkeley: Pacific Earthquake Engineering Research Center, 2001, 6-7.